Electronic Supplementary Material (ESI) for Journal of Materials Chemistry A.

Graphene nanoscroll based Janus bifunctional separators of suppressing lithium dendrites and polysulfides shuttling synchronously for high performance lithium sulfur batteries

Zhigang Zhang[a], Yanfeng Dong[b,c], Yuefeng Gu[a], Pengfei Lu[b], Fangfang Xue[a], Yangtao Fan[a], Zhicheng Zhu[a], Jun Lin[a], Qiuhong Li[a,*], Zhong-Shuai Wu[b]

[a]Pen-Tung Sah Institute of Micro-Nano Science and Technology, Xiamen University, Xiamen 361005, China. E-mail: liqiuhong@xmu.edu.cn

[b]State Key Laboratory of Catalysis, Dalian Institute of Chemical Physics, Chinese Academy of Sciences, 457 Zhongshan Road, Dalian 116023, China.

[c]Department of Chemistry, College of Sciences, Northeastern University, Shenyang 110819, China.

Synthesis of 20 nm Co_3O_4 nanoparticles: In a typical procedure, 0.5 g $Co(CH_3COO)_2 \cdot 4H_2O$ was dissolved in 25.0 mL DI water, and 3 mL 25% ammonia was added under vigorous stirring. The mixture was stirred in air for about 30 min to form a homogeneous fuscous slurry. Then the suspension was transferred into a 48.0 ml autoclave, sealed and maintained at 150 °C for 4 h. After this, the autoclave was cooled to room temperature naturally. The resulting black solid products were washed with water via centrifugation–redispersion, dried at 60 °C for 4 h, and collected for characterization.

Synthesis of Co_3O_4@GNS composite: For preparation of Co_3O_4@GNS, 30 mg sodium dodecyl benzene sulfonate (SDBS) was added to modify Co_3O_4 aqueous dispersion (1.0 mg mL^{-1}, 100 mL) with appropriate mechanical stirring and sonication. Then GO suspension (1.0 mg mL^{-1}, 50 mL) and the modified Co_3O_4 aqueous dispersion (1.0 mg mL^{-1}, 50 mL) were mixed together with the aid of sonication for 10 min. The mixed suspension was transferred to centrifuge tubes which was heated up to 80 °C, and then the tubes were put into liquid nitrogen to make Co_3O_4@GONS. Then the

completely frozen solid composite material was suffered vacuum freeze-drying to remove water.

Synthesis of CoS_2@GNS composite: In a typical synthesis, the as-obtained Co_3O_4@GONS powder and sulfur powder were loaded in two different combustion boat. A glass plate was partially covered on the combustion boat with the downstream side opening. Argon gas (500 sccm) was initially flowed into the tube for 1 hour to remove the air. Then, the samples were annealed at 400 °C for 3 h with a heating rate of 2 °C min^{-1} under Argon atmosphere with a flow rate of 400 sccm. The CoS_2@GNS composites were obtained after cooling to ambient temperature. The black solid products were rinsed with carbon disulfide and then harvested by centrifugation with DI water and ethanol for several times. Finally, the purified CoS_2@GNS nanomaterials are dried at 60 °C under vacuum state for 6 h.

Synthesis of NGNS material: Then the GO suspension (0.5 mg mL^{-1}, 100 mL) and 20 mg sodium citrate were mixed together with aid of sonication for 10 min. The mixed suspension was transferred to centrifuge tubes which was heated up to 80 °C, and then the tubes were put into liquid nitrogen to make pure GONS. The N-GNS solid powder was obtained by thermal treatment at 500 °C for 1 h with a heating rate of 8 °C min^{-1} in ammonia/argon atmosphere.

Electrochemical characterization: The cells were assembled in an argon-filled glove box with water and oxygen content below 0.5 ppm. The electrochemical performance of Li-S batteries was studied using CR2032 coin cells with lithium foil as the counter and reference electrode. The CoS_2@GNS/S electrode was cut into thin circular plates

with diameter of 12 mm as working electrode. And the areal loading of S loaded in the electrode was 2.7 mg cm^{-2}.The electrolyte was 1.0 M LiTFSI in a mixture solution of 1,3-dioxolane (DOL) and 1,2-dimethoxyethane (DME) (1:1, vol. ratio) with 1 wt % $LiNO_3$ as additive. The cells were firstly discharged to 1.7 V, and then cycled between 1.7 and 2.8 V at different rates. The galvanostatic discharge-charge (GCD) profiles were performed using a LAND CT2001A battery system. CV curves were carried out on a CHI660E electrochemical workstation at a scan rate of 0.1 mV s^{-1}. Electrochemical impedance spectroscopy (EIS) measurements were performed by Zennium electrochemical workstation at a frequency range from 0.01 Hz to 100 kHz with an AC perturbation signal of 5 mV.

Material Characterization: The crystal structure of the materials was investigated by a powder X-ray diffraction (XRD) system (Rigaku Ultima IV) with Cu Ka radiation from 10° to 80° (2θ) at a scan rate of 10° min^{-1}. Field-emission scanning electron microscopy (FESEM, SUPRA-55, ZEISS, Germany), elemental mapping was performed on a FESEM equipped with an Oxford INCA energy dispersive spectrometer (EDS). Transmission electron microscopy (TEM, JEOL JEM2100) was used to detect the morphology and microstructure. The contents of carbon and sulfur in the samples were evaluated by elementary CHN combustion analysis. Thermogravimetric analysis (TGA) was performed in air at 10 °C min^{-1} from room temperature to 600 °C on a Perkin-Elmer instrument.

Theoretical Calculations: The Density Functional Theory (DFT) calculations were conducted by Vienna ab initio simulation package (VASP) code. Electron-ion

interactions were described by using projector augmented wave. Firstly, the optimum geometries of pyridinic N (pN), pyrrolic N and graphitic N in graphene substrate models were calculated with generalized gradient approximation (GGA) method in the Perdew-Burke-Enzerhof (PBE) level. The effective core potentials were considered when tackling the electron-ion interactions in the whole system. The minimum allowed energy change between the two adjacent iterative steps was set to 2×10^{-5} Ha, the force and displacement tolerances were set to 0.004 Ha/Å and 0.005Å, respectively. To understand the interaction strength between Li ions and different substrates, the binding energy (Eb) was defined as $E_b = E_{total} - E_{sub} - E_{Li}$, where Etotal is the total energy of the whole adsorbed system, E_{sub} is the energy of the substrate materials and E_{Li} is the energy of the Li atom in a Li crystal.

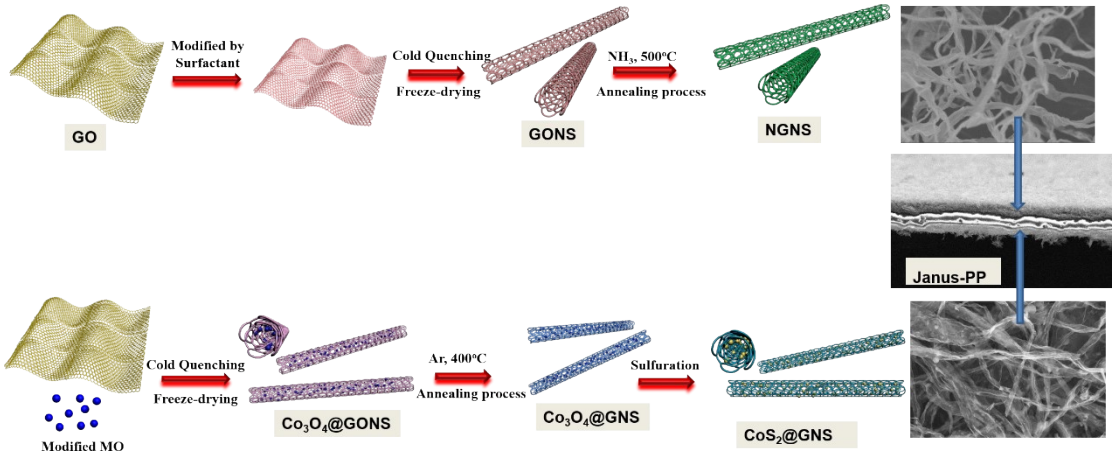

Figure S1. Preparation of Janus-PP separator.

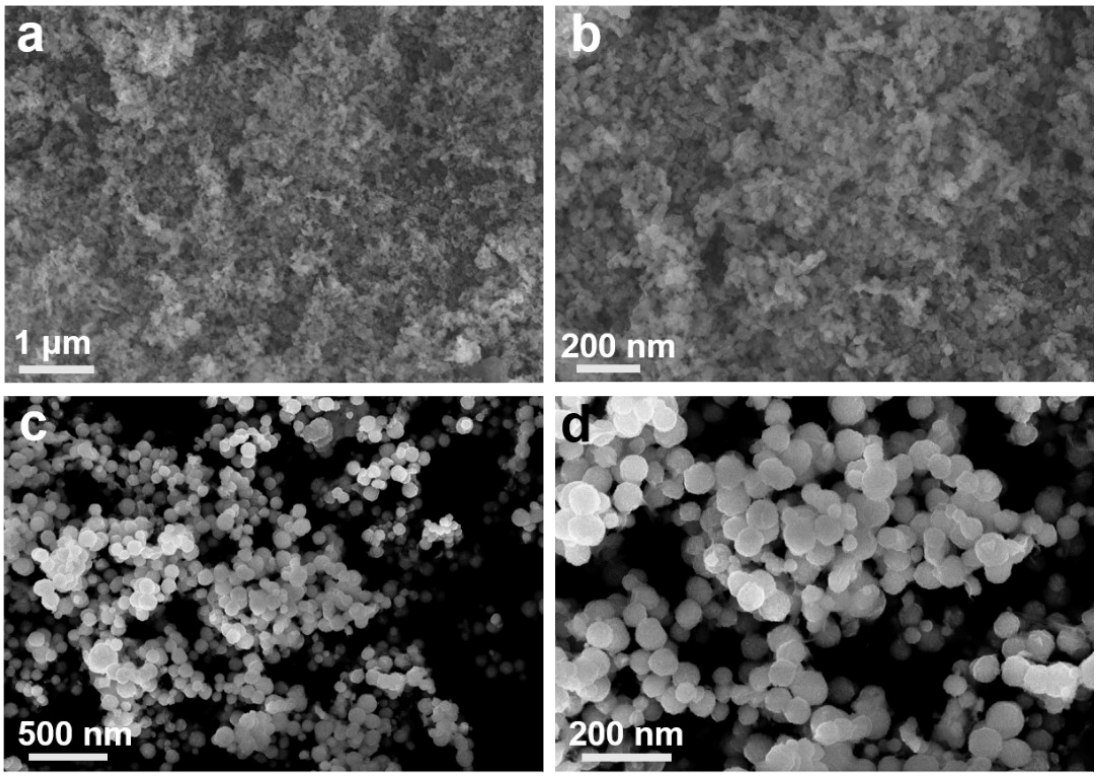

Figure S2. SEM images of (a, b) Co_3O_4 (20 nm), (c, d) Co_3O_4 (100 nm).

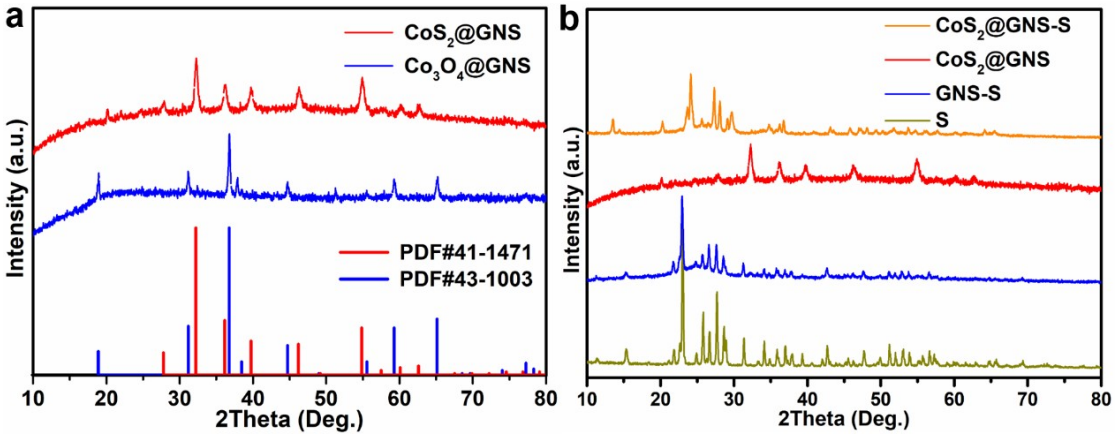

Figure S3. XRD patterns of **(a)** GNS@Co_3O_4 and GNS@CoS_2 composite materials, **(b)** pristine sulfur, GNS@CoS_2, GNS/S electrode, and GNS@CoS_2/S electrode.

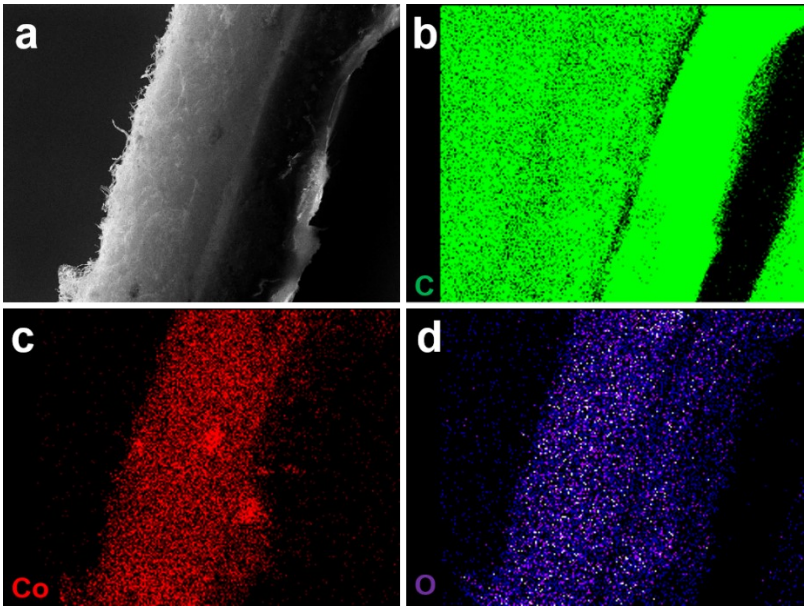

Figure S4. Side-view and corresponding EDX elemental mapping images of the Co-PP seperator.

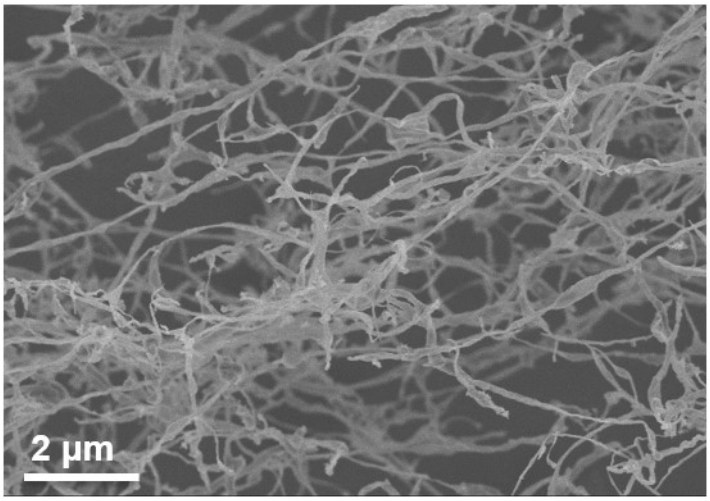

Figure S5. SEM image of NGNS

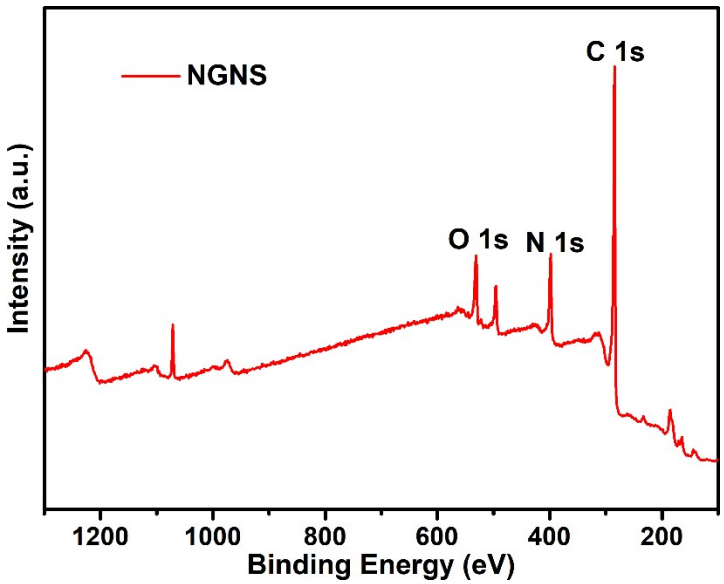

Figure S6. XPS survey spectrum of NGNS.

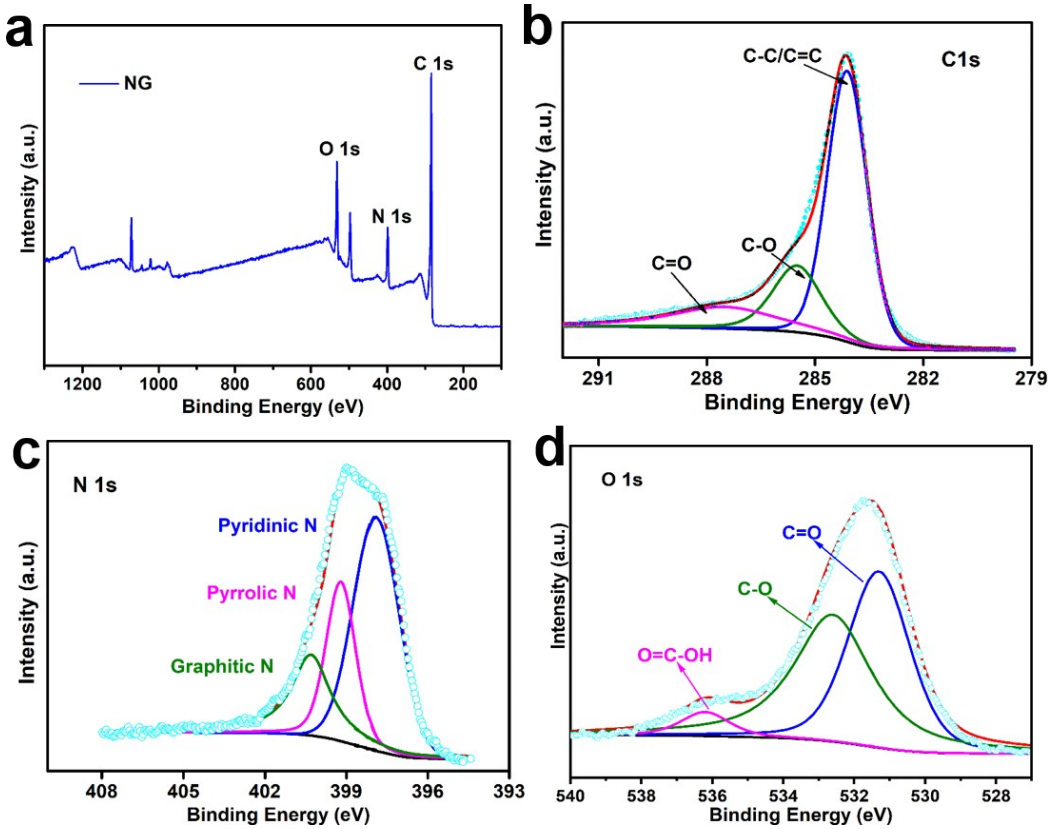

Figure S7. XPS survey spectrum of NG. High resolution XPS spectrum of C 1s spectra (b), N 1s spectra and O 1s spectra in NG.

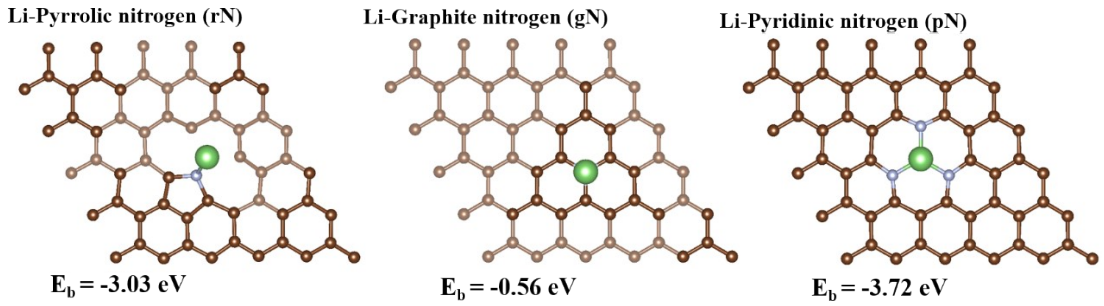

Figure S8. The optimized binding energies of a Li atom and different heteroatom-doped graphene.

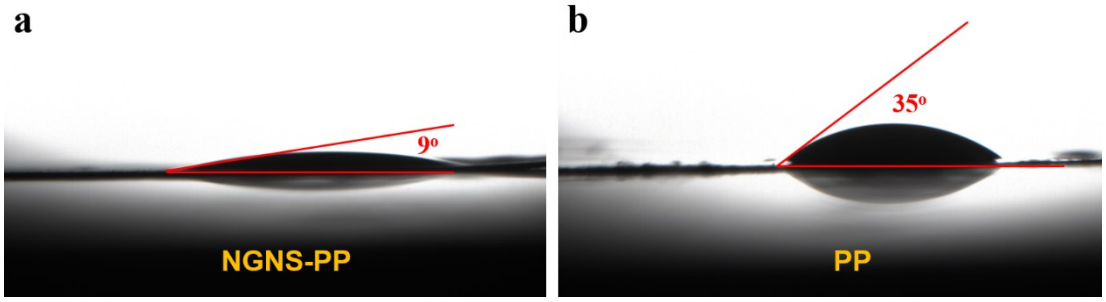

Figure S9. Contact angles of the electrolyte on NGNS-PP and bare PP separators.

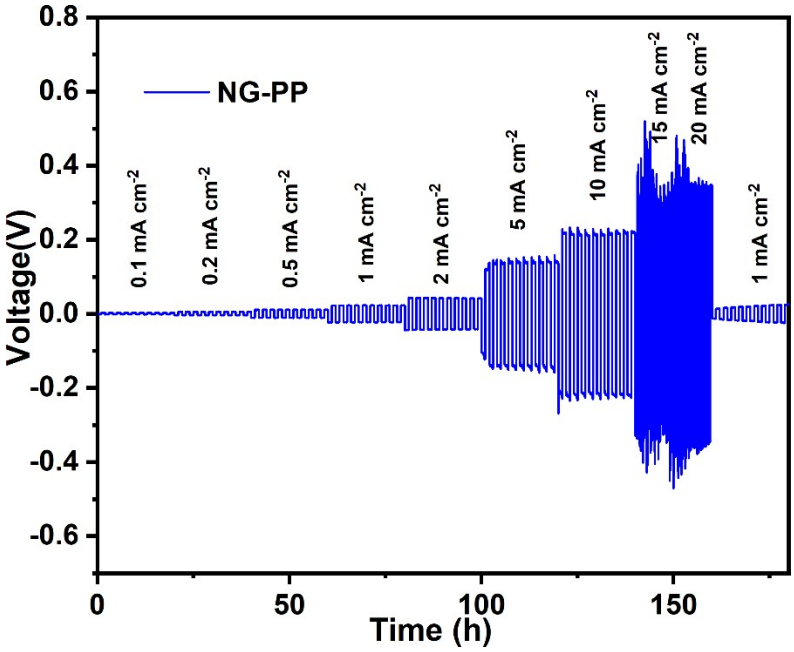

Figure S10. Li plating/stripping behavior of Li//Li symmetric cell with N-GNS separator at various current densities from 0.5 to 20 mA cm^{-2}.

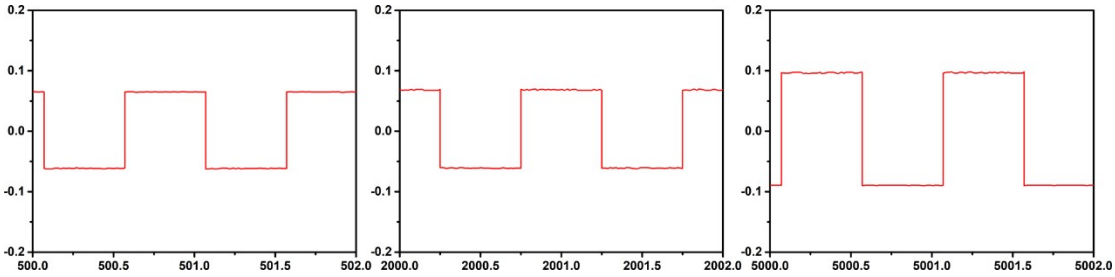

Figure S11. Detailed voltage hysteresis of Li//Li symmetric cell at a high current density of 10 mA cm^{-2} with areal-capacity of 5 mA h cm^{-2}.

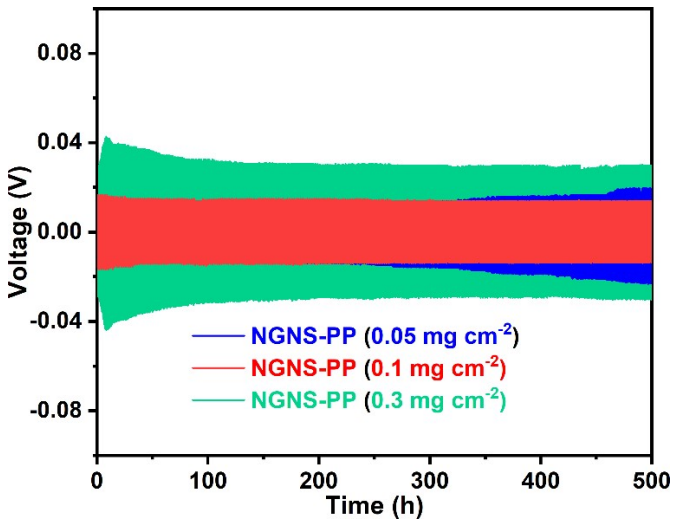

Figure S12. Voltage profiles of Li-Li cells with NGNS-PP separators of different mass loading at current density and capacity of 3 mA cm^{-2} and 1 mA h cm^{-2}.

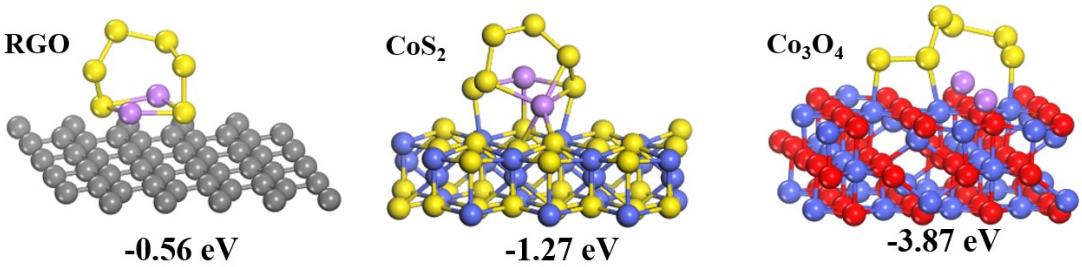

Figure S13. Adsorption configurations and energies of L_2S_6 (A) on RGO, Co_3O_4 and CoS_2 based compounds.

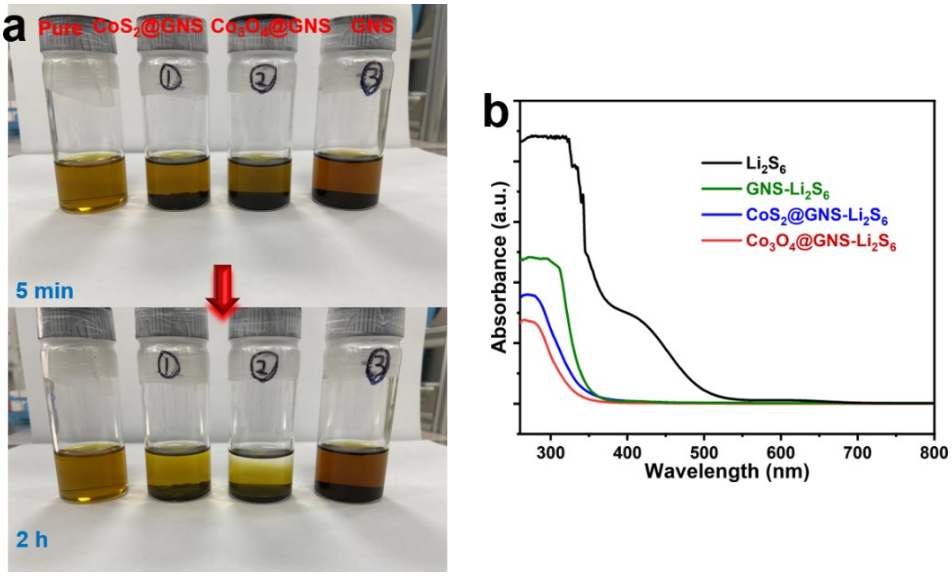

Figure S14. Lithium polysulfide adsorption test: (a) physical appearances of Li_2S_6 solution (Li_2S_6 in DOL/DME solvent) containing Co_3O_4@GNS, CoS_2@GNS, and GNS samples after 5 min and 2 h; (b) UV–vis spectra of the resultant Li_2S_6 solution with different samples.

The adsorption capability of Co_3O_4@GNS, CoS_2@GNS, and GNS samples with polysulfides was experimentally evaluated by adding 10 mg of the sample into mixed dioxolane/dimethoxyethane (DOL/DME, 1:1 in volume) solution of 0.01 M Li_2S_6 (Figure S14). The Li_2S_6 solutions mixed with Co_3O_4@GNS turned from yellow to almost colorless within 2 h, while the Li_2S_6 solution mixed with CoS_2@GNS only displays slight decoloration, confirming the high adsorption ability of Co_3O_4 to sulfur species. UV-visible absorption spectra were further used to investigate the Li_2S_6 concentration changes in the solutions after adding Co_3O_4@GNS, CoS_2@GNS, and GNS samples (Figure S14b). The solution soaked with Co_3O_4@GNS shows much weaker polysulfide characteristic absorption peaks as compared to those soaked with GNSs and CoS_2@GNS samples, further proving that the Co_3O_4@GNS can effectively trap the migration of polysulfides. This ability in trapping polysulfides could be attributed to the strong polar affinity of the Co_3O_4.

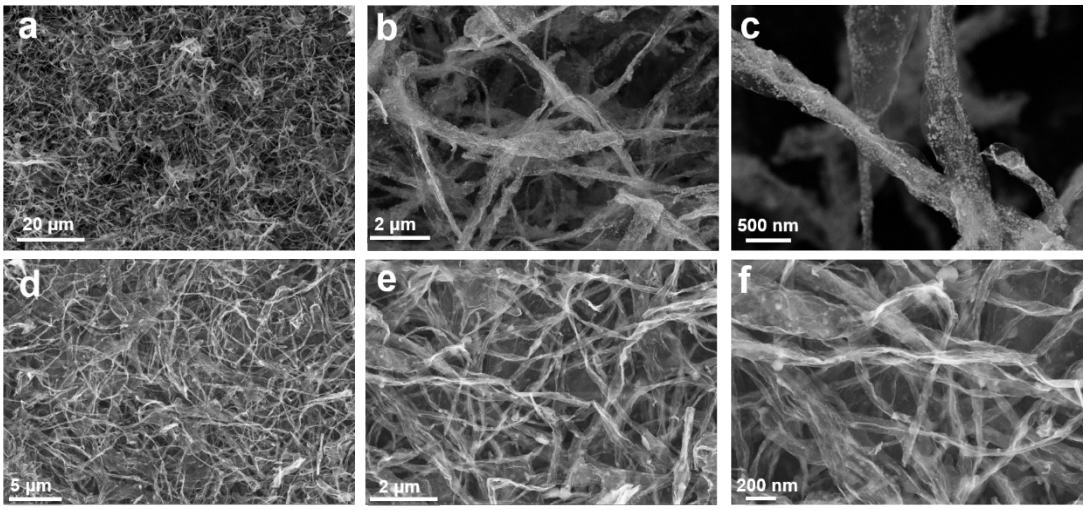

Figure S15. SEM images of (a-b) Co_3O_4@GNS, (d-f) CoS_2@GNS.

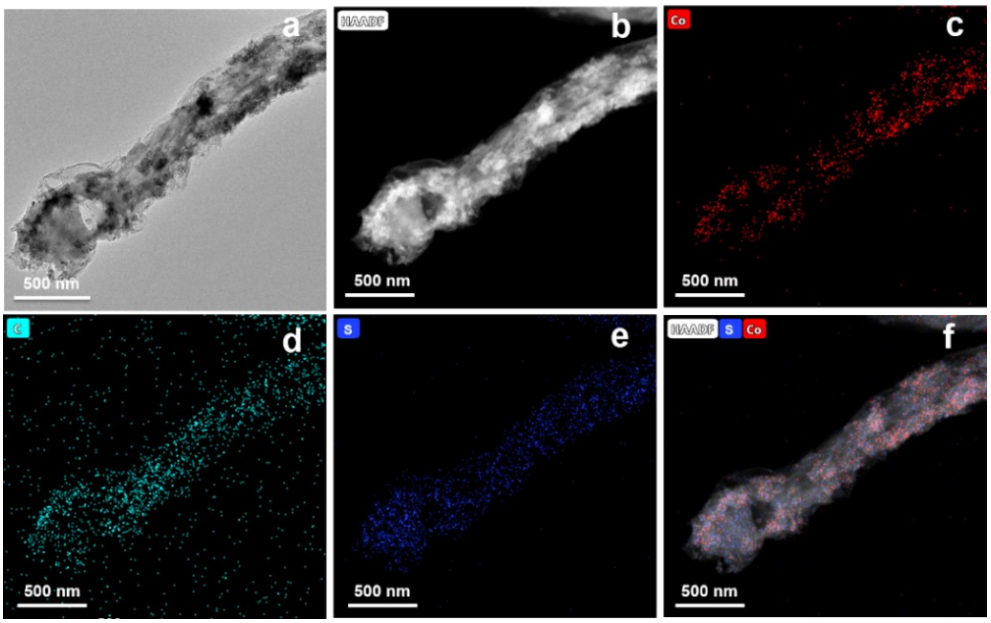

Figure S16. TEM image (a), STEM image (b) and corresponding EDX elemental mapping of cobalt (red), carbon (green) and sulfur (blue) of their overlay with the STEM image (f) of CoS_2@GNS composites.

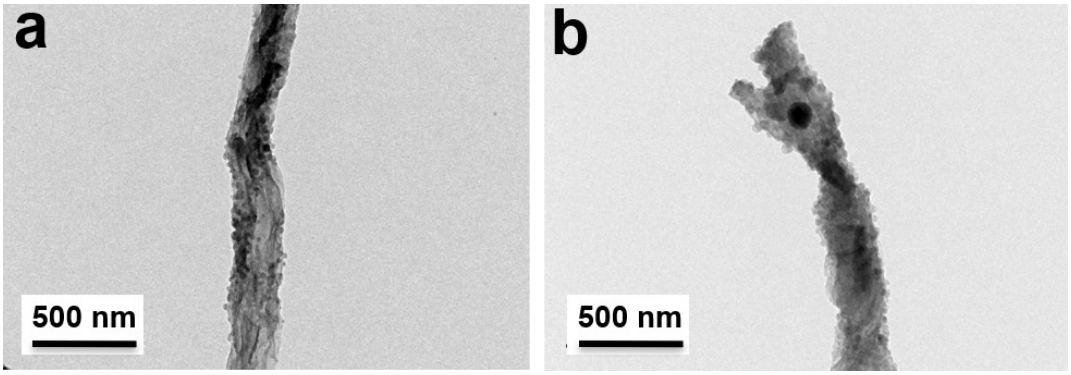

Figure S17. TEM images of CSG/S composites.

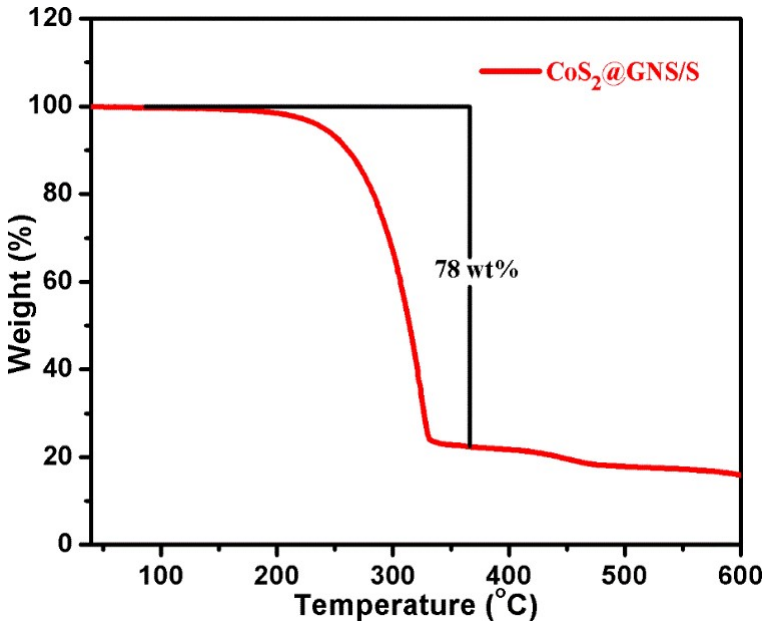

Figure S18. The thermogravimetry (TG) curve of CSG/S with S feeding ratio of 78 wt %.

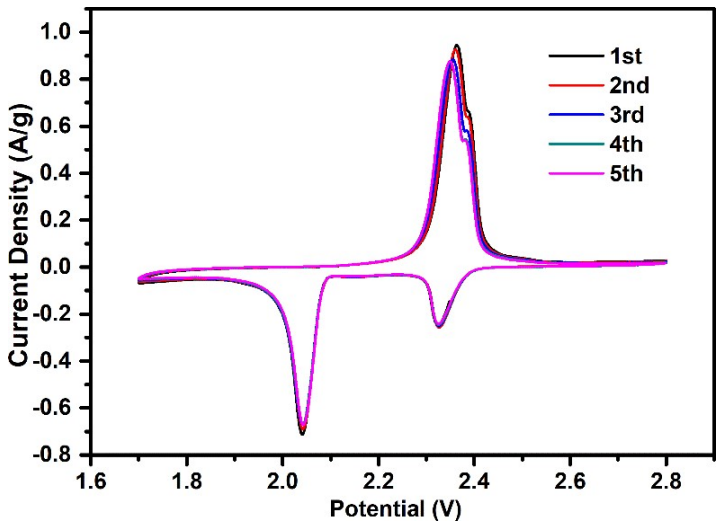

Figure S19. The CV curves of CSG/S-Janus PP electrode measured at the initial five cycles, tested at 0.1 mV s^{-1}

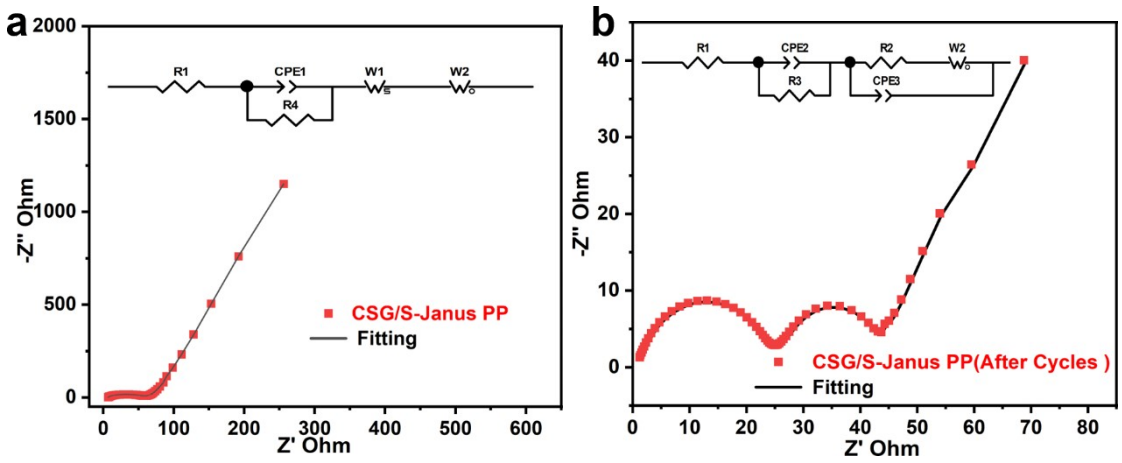

Figure S20. EIS spectra of CSG/S-Janus PP Li-S batteries (a) before and (b) after running the battery at 1 C for 50 cycles.

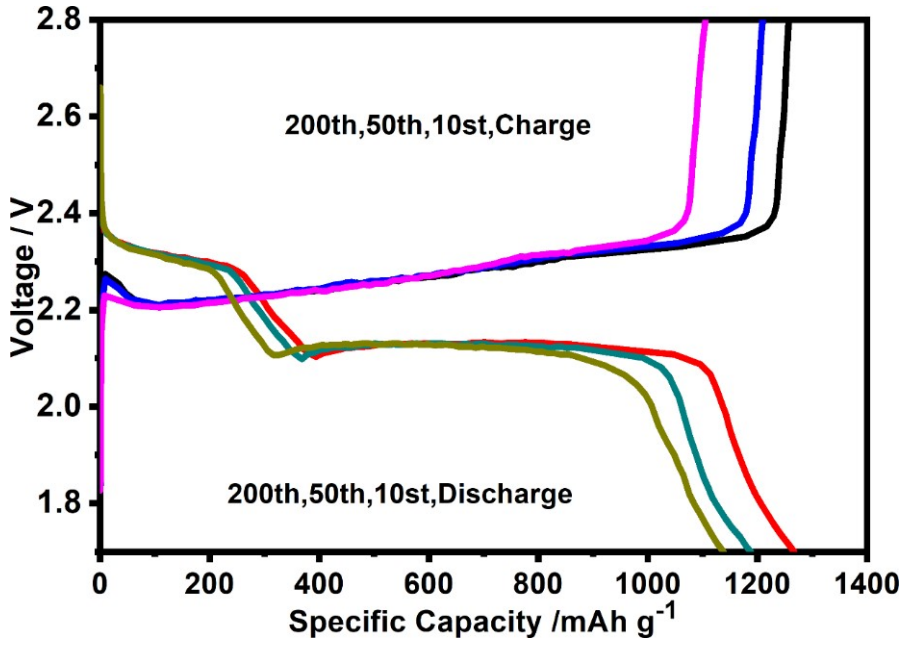

Figure S21. GCD profiles obtained at 0.2 C of CSG/S-Janus PP.

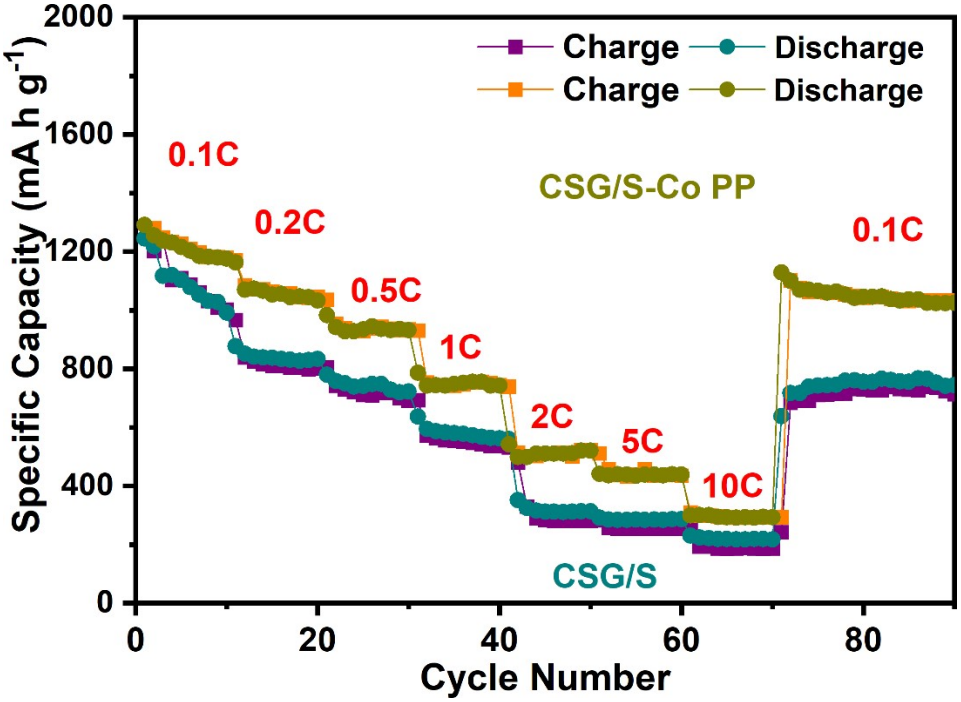

Figure S22. Rate capability of CSG/S-Co PP and CSG/S cathode cycled at different current densities from 0.1 C to 10 C (0.1, 0.2, 0.5, 1.0, 2.0, 5.0 and 10 C)

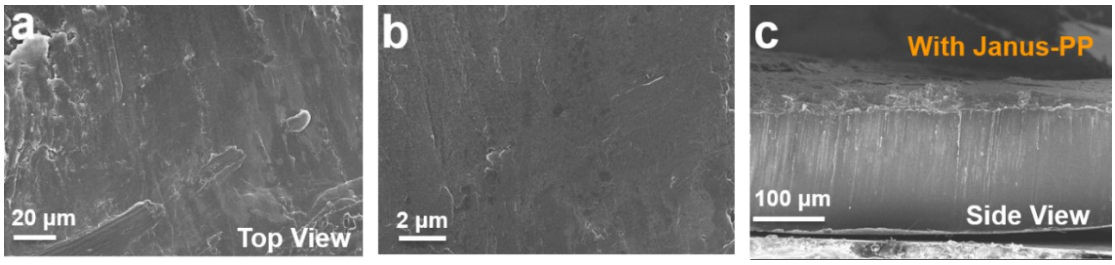

Figure S23. Top-view and side-view SEM images for the cycled Li-metal anode with the CSG/S-Janus PP.

Table S1. Elemental composition of NGNS and NG.

Element	NG (Atomic %)	NGNS (Atomic %)
C	78.89	72.12
N	11.63	14.78
O	9.48	13.10